Article

# Synthesis of Magnesium Hydroxide and Oxide Nanoparticles Using a Spinning Disk Reactor

Clifford Y. Tai, Chia-Te Tai, Ming-Hui Chang, and Hwai-Shen Liu

*Ind. Eng. Chem. Res.*, **2007**, 46 (17), 5536-5541 • DOI: 10.1021/ie060869b

MATERIALS AND INTERFACES

# Synthesis of Magnesium Hydroxide and Oxide Nanoparticles Using a Spinning Disk Reactor

**Clifford Y. Tai,* Chia-Te Tai, Ming-Hui Chang, and Hwai-Shen Liu**

*Department of Chemical Engineering, National Taiwan University, No. 1, Section 4, Roosevelt Road, Taipei, Taiwan*

The aim of this research was to synthesize magnesium hydroxide nanoparticles, which were further calcined to form magnesium oxide, using a spinning disk reactor. Magnesium hydroxide was prepared by continuously pumping two aqueous solutions of $MgCl_2$ and NaOH, respectively, into the chamber of the reactor, where a liquid−liquid reaction took place to form $Mg(OH)_2$. The effects of various operating variables, including the rotation speed, reactant concentration, and liquid flow rate of the reactants, on the size of magnesium hydroxide nanoparticles were investigated. The particle size of magnesium hydroxide increased as the flow rate increased, but remained quite constant as the reactant concentration varied. As far as size and uniformity were concerned, the best lamellar magnesium hydroxide particles were 50−80 nm in length and 10 nm in thickness. The particle morphology and size of magnesium oxide calcined from produced magnesium hydroxide were also analyzed. Polyhedral nanoparticles of 30−70 nm magnesium oxide were obtained by calcinating lamellar hydroxide.

## 1. Introduction

Magnesium hydroxide, so-called brucite, is usually used in flame retardant composite formulations because of its ability to undergo endothermic dehydration in fire conditions.[1] It can also be used to neutralize acid waste streams and to treat flue gases, thus providing cost-effective solutions to environmental problems.[2] In industry, it can be produced by reacting alkali solutions with magnesium chloride contained in seawater or natural brines, and used as a precursor for manufacturing magnesium oxide.[3] Crystalline magnesium hydroxide is hexagonal in structure, with a layered $CdI_2$-type arrangement.[4] This arrangement is advantageous for the formation of platelet-shaped crystals. When the particle size of $Mg(OH)_2$ is in the nano range, its platelet shape can enhance the mechanical reinforcement of its composite, i.e., inorganic $Mg(OH)_2$ dispersed in a polymer matrix.[1] Many methods for synthesizing magnesium hydroxide nanoparticles, including the precipitation method,[1,5] hydrothermal method,[6,7] and sol−gel method,[8,9] have been developed, but most of them are in laboratory scale. Furthermore, these methods are time-consuming or expensive and difficult to scale up.

Magnesium oxide is one of the most useful ceramic materials. Because of its high melting temperature (about 2800 °C), it is usually used in fire-resisting bricks or crucibles. It is also an exceptionally important material for use in catalysis and toxic waste remediation, or as an additive in paint and superconductor products.[7] The crystal structure of magnesium oxide is cubic, which makes it a periclase structure.[4] Its atomic arrangement is of the NaCl type, and this arrangement causes the common morphologies of MgO to be cubic, octahedral, and polyhedral in shape.[10] Magnesium oxide can be produced through the decomposition of magnesium hydroxide or magnesium carbonate.[9,11−13] Because the preparation of magnesium oxide involves a calcination process, it is difficult to keep the particle size in the nano range.

Ding et al.[7] prepared magnesium hydroxide via a hydrothermal method using different magnesium precursors, such as magnesium powder and magnesium sulfate, from different solvents, including ethylenediamine and NaOH solution. Magnesium hydroxide nanoparticles with rod-like, lamellar-like, and needle-like morphologies were obtained by varying the reaction time from 2 to 20 h and the reaction temperature from 80 to 110 °C. These 20−200 nm magnesium hydroxide nanoparticles were further calcinated at temperatures up to 450 °C, where 20 nm magnesium oxide particles with lamellar-like and needle-like morphologies appeared. Utamapanya et al.[9] synthesized magnesium hydroxide by means of a sol−gel method. Magnesium hydroxide gel was obtained when $Mg(OCH_3)_2$ was reacted with water in a methanol−toluene solvent mixture. Then the gel was subjected to a modified hypercritical drying procedure to get magnesium hydroxide, which had a surface area of 1000 $m^2/g$ and a crystallite size of 3.5 nm, as determined from X-ray diffraction patterns. It was further calcined at 500 °C to obtain magnesium oxide nanoparticles, which were about 8 nm in size and had a 300−400 $m^2/g$ surface area. The study demonstrated possible methods for synthesizing magnesium hydroxide and oxide nanoparticles. However, the procedure used to synthesize and handle the hazardous metal−organic precursors in the sol−gel process was not very convenient.

Higee equipment has been developing for many years.[14] There are two types of devices, i.e., the high-gravity rotating packed-bed reactor (RPBR) and the spinning disk reactor (SDR). In recent years, they have been successfully applied in distillation,[15] adsorption,[16] and absorption processes.[17,18] In the field of crystal engineering, Higee technology can be used to produce nanoparticles.[19−21] In an RPBR, which functions similarly to a combined static mixer and stator−rotator mixer, the fluids going through the packing are spread or split into very fine droplets, threads, and thin films under a high shear force. The mass-

* To whom correspondence should be addressed. Tel.: 886-2-23620832. Fax: 886-2-23623040. E-mail: cytai@ntu.edu.tw.

10.1021/ie060869b CCC: $37.00 
Published on Web 07/21/2007

transfer rate is higher than that in a conventional packed bed, and this is very helpful for achieving high supersaturation in a precipitation process.[19] Lamellar-like magnesium hydroxide nanoparticles, 20−80 nm in mean particle size, were successfully synthesized by Song et al.[20] through the reaction of a magnesium chloride solution with an ammonium hydroxide solution or gaseous ammonia in an RPBR at temperatures between 60 and 160 °C.

Compared with an RPBR, an SDR is a simpler type of equipment, in which the liquid spreads over a disk to form a thin film due to the high centrifugal force caused by spinning. Cafiero et al.[21] have precipitated barium sulfate in an SDR by reacting a barium chloride solution with a sodium sulfate solution. The micromixing time in an SDR was calculated to be 0.9 ms under a rotation speed of 900 rpm, and this was shorter than the induction time of the barium sulfate, which was about 2.65 ms with a supersaturation ratio of 1272. This could provide uniform supersaturation in the reactor and enhance homogeneous nucleation so that uniform distribution of the particle size was obtained. It was also shown that the SDR did not require as much power as a traditional continuous reactor to push the stirrer in the liquid. The difference was about 1000 times. Furthermore, the SDR was shown to be a valid candidate for use in precipitation processes in industrial applications with a very high production rate, and scale-up of the device was not as problematic as that of a rapid T-mixer, which was used by Mohanty et al.[22] to produce $BaSO_4$ particles.

The purpose of this research was to synthesize magnesium hydroxide nanoparticles in a spinning disk reactor and then use them as precursors for preparing magnesium oxide. The effects of various operating variables, including the rotation speed, reactant concentration, and liquid flow rate of the reactants, on the particle size and shape of magnesium hydroxide particles were studied. In addition, based on the information obtained from differential thermal analysis, magnesium hydroxide produced by this technique was calcined to form magnesium oxide, which was then analyzed with an X-ray diffractometer and a scanning electron microscope to determine its morphology and crystal structure.

## 2. Experimental Section

A schematic diagram of the Higee system used in this study is shown in Figure 1. It consists of a liquid feeding system, a spinning disk reactor, and a slurry collection vessel. The liquid feeding system contains two tanks (1 and 2), from which liquid reactants are pumped into the reactor chamber through a flowmeter (4) and a liquid distributor (8). The two liquid distributors, which are straight tubes 4.5 cm in length with a 3 mm hole at the end, are set up parallel to each other and 7 mm apart, and perpendicular to the spinning disk (9) at a distance of 5 mm. The main part of the spinning disk reactor (5) is a stainless steel disk (9), 12 cm in diameter, driven by a variable-speed motor (6). The spinning disk is enclosed in a cylindrical acrylic chamber 15 cm in diameter and 6 cm deep. A funnel-like outlet is located at the bottom of the chamber for guiding the slurry into the collection vessel (7).

The chemical reactions involved in the formation of magnesium hydroxide and oxide are as follows:

$$MgCl_2(aq) + 2NaOH(aq) \rightarrow Mg(OH)_2(s)\downarrow + 2NaCl(aq) \quad (1)$$

$$Mg(OH)_2(s) \xrightarrow{\Delta} MgO(s) + H_2O(g)\uparrow \quad (>350\ ^\circ C) \quad (2)$$

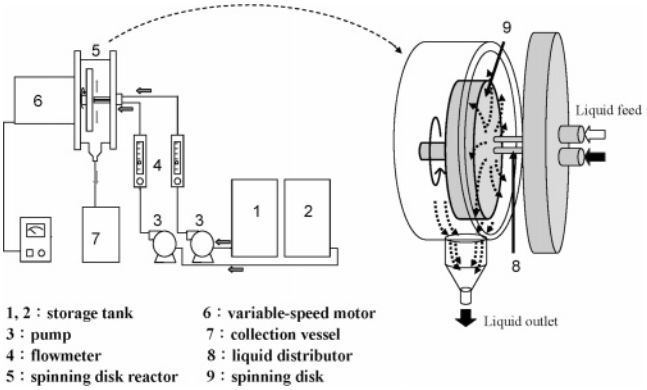


**Figure 1.** Experimental apparatus.

At the beginning, 1-L magnesium chloride and sodium hydroxide solutions with concentrations ranging from 0.20 to 1.92 M were charged separately into tanks 1 and 2. The two reactant solutions were pumped onto the center of the spinning disk (with a rotation speed $N$) through the two distributors at a controlled flow rate ($L_1$ and $L_2$). Then the liquid was accelerated due to centrifugal force, causing it to spread over the disk surface and forming a thin film where the $Mg(OH)_2$ precipitation reaction took place. The slurry containing $Mg(OH)_2$ particles left the disk, hit the inner wall of the chamber, flowed down along the wall past the funnel-like outlet, and finally collected in the vessel. The product slurry was centrifuged at 10 000 rpm for 10 min, washed with deionized water and 99.5% ethanol, dried at 60 °C for 1 day, and milled with a ceramic mortar to obtain $Mg(OH)_2$ powder. Part of the produced $Mg(OH)_2$ powder was subjected to a calcination process for producing MgO powder.

Powder samples were then analyzed with an X-ray diffractometer (XRD; Mac Science, MXP-3TXJ-7266) using Cu Kα ($\lambda = 1.5418$ Å) radiation to determine their crystal structures. Morphologies of particles were observed with a scanning electron microscope (SEM; JEOL J-5600) and a field-emission gun scanning electron microscope (FEG-SEM; Philips Tecnai, F30). To determine the particle size distribution, $Mg(OH)_2$ powder was dispersed in water with a sonicator (Misonix, XL2020), using poly(acrylic acid, sodium salt) (MW 2100, Sigma-Aldrich, Inc.) and sodium hexametaphosphate (Kokusan Chemical Works, Ltd.) as dispersants, and was analyzed with a dynamic light scattering analyzer (Zeta-sizer, Malvern $3000HS_A$). Unlike the $Mg(OH)_2$ powder, MgO powder was dispersed in methanol, without adding any surfactant or dispersant. The dehydration temperature of $Mg(OH)_2$ was determined by a differential thermal analyzer (DTA; Ulvac/Riko, TGD-7000HD) using air atmosphere with a flow rate of 100 mL/min, and the rate of temperature increase was 10 °C/min. The specific surface area was determined from nitrogen adsorption data at liquid nitrogen temperature using the BET technique (Micromeritics, ASAP-2000).

## 3. Results and Discussion

**3.1. Effects of Reactant Concentration on $Mg(OH)_2$ Particle Size.** To investigate the effects of the reactant concentration on the $Mg(OH)_2$ particle size, other operating variables were fixed: the liquid flow rates of $MgCl_2$ and NaOH solution were set at 0.28 L/min, the spinning disk rotated at 2000 rpm, and the $[MgCl_2]/[NaOH]$ ratio was kept at 1/2 according to the stoichiometric ratio of the reaction. As the $MgCl_2$ concentration, $[MgCl_2]$, varied from 0.20 to 0.92 M and

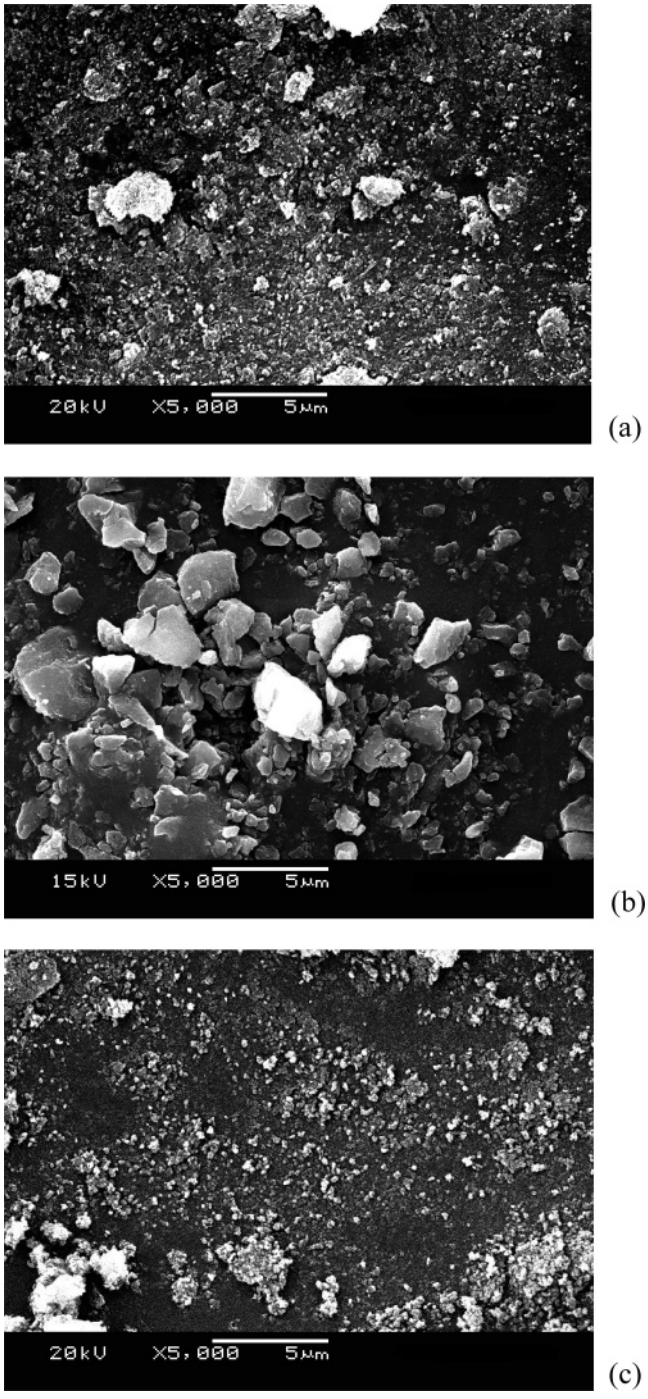


**Figure 2.** SEM micrographs of $Mg(OH)_2$ particles produced under different $[MgCl_2]/[NaOH]$ ratios and specific conditions at $L_1 = L_2 = 0.28$ L/min and $N = 2000$ rpm: (a) 1/2, (b) 1/4, and (c) 1/1.

[NaOH] varied from 0.40 to 1.84 M, the concentrations of the reactants had no significant effect on the number mean size of $Mg(OH)_2$, which changed from 40.0 to 47.5 nm. This might be due to the very high degree of supersaturation (about 400−3000) generated in this experiment for all the concentrations studied. Under these conditions, the main action was the very fast primary nucleation, so the particles were very small. On the other hand, the change in the volume mean size from 54.6 to 71.8 nm was noticeable. It may have been caused by slight agglomeration. Concentrations lower than 0.20 M were not investigated, because the production rate was too low to be practical.

**3.2. Effects of Disk Rotation Speed on $Mg(OH)_2$ Particle Size.** In this section, the effects of the rotation speed of the disk on the $Mg(OH)_2$ particle size are discussed as the other operating variables stayed constant. As the rotation speed increased from 400 to 2000 rpm, the number mean size decreased from 58.0 to 47.5 nm, and the volume mean size decreased from 80.2 to 62.7 nm. It could be concluded that, at a high rotation speed, efficient mixing on the disk was achieved, resulting in uniform, high supersaturation and enhancing the agitation within the film. Thus, smaller crystals with less aggregation were produced. Similar results have been reported by Cafiero et al.[21] They investigated the effects of the disk rotation speed on $BaSO_4$ particle sizes. When the disk rotation speed increased from 200 to 1000 rpm, the average crystal size of $BaSO_4$ evaluated from transmission electron micrographs decreased from 3.0 to 0.7 $\mu$m.

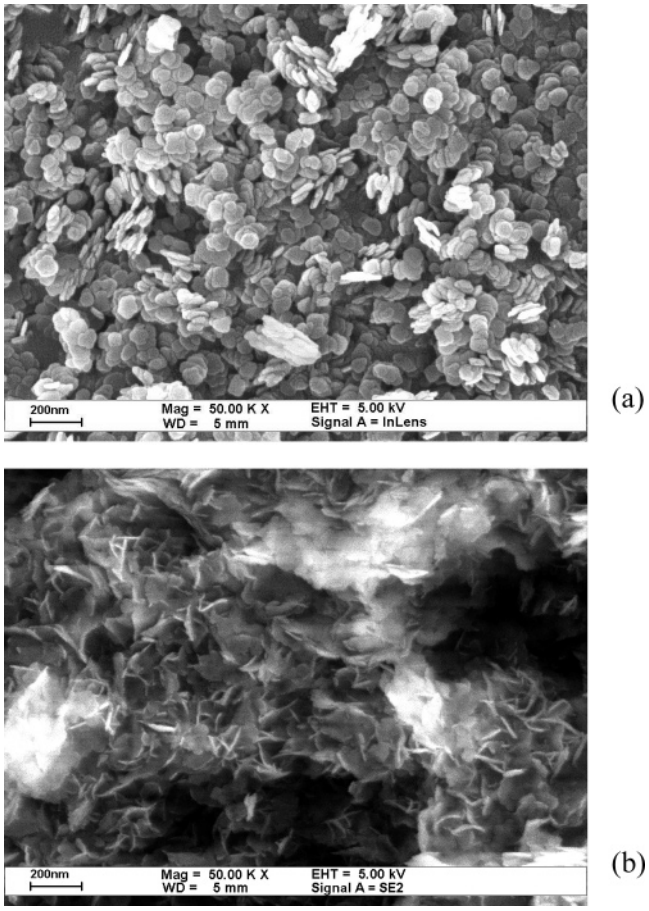


**Figure 3.** FEG-SEM micrographs of $Mg(OH)_2$ particles produced from different magnesium sources, (a) 0.83 M $MgCl_2 \cdot 6H_2O$ and (b) 0.80 M $MgSO_4 \cdot 7H_2O$, which reacted with NaOH solution under the following specific conditions: $[Mg^{2+}]/[NaOH] = 1/2$, $L_1 = L_2 = 0.28$ L/min, and $N = 2000$ rpm.

**3.3. Effects of Reactant Concentration Ratio on $Mg(OH)_2$ Particle Size.** The reactant concentration ratio or molar ratio of the reactants could influence the particle size. In the reverse microemulsion system for synthesizing $CaCO_3$, different molar ratios of reactants altered the pH value of the solution and gave different particle sizes as reported by Chen.[23] In this experiment, the concentration ratio of $MgCl_2$ to NaOH was set at 1/1, 1/2, and 1/4 to determine the effects of the concentration ratio on the $Mg(OH)_2$ particle size. When the $[MgCl_2]/[NaOH]$ ratio was 1/2, which is the stoichiometric ratio of the reaction, the pH value of the exit stream from the reactor was about 10.0, which was approximately the pH value of the saturated $Mg(OH)_2$ solution. When the $[MgCl_2]/[NaOH]$ ratio was changed to 1/4 and 1/1, the pH values of the $Mg(OH)_2$ slurry were about 13.2 and 9.8, respectively. The pH value of the former, which was

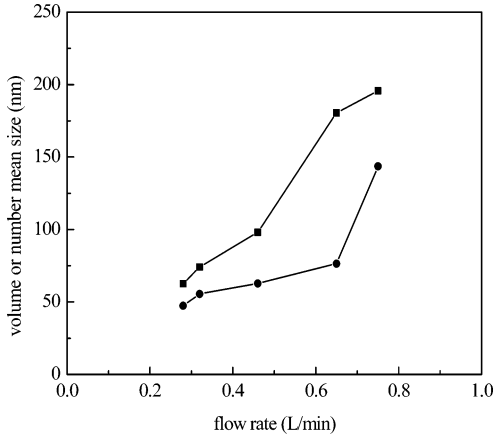


**Figure 4.** Effects of $MgCl_2$ solution flow rate on the number mean size (●) and volume mean size (■) of $Mg(OH)_2$. Operating conditions: $[MgCl_2] = 0.83$ M, $[NaOH] = 1.66$ M, $L_1/L_2 = 1/1$, and $N = 2000$ rpm.

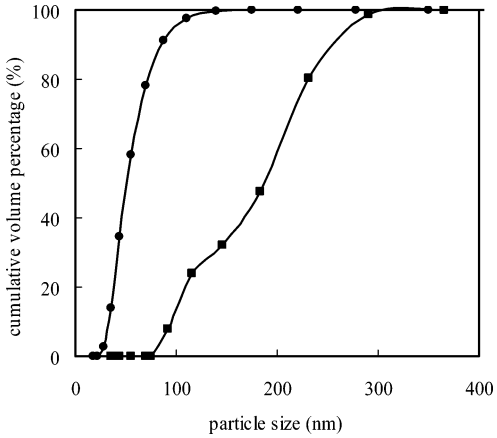


**Figure 5.** Cumulative particle size distribution on a volume basis of the samples obtained at different reactant flow rates: (●) $L = 0.28$ L/min and (■) $L = 0.75$ L/min. Other operation conditions were $[MgCl_2] = 0.83$ M, $[NaOH] = 1.66$ M, $L_1/L_2 = 1/1$, and $N = 2000$ rpm.

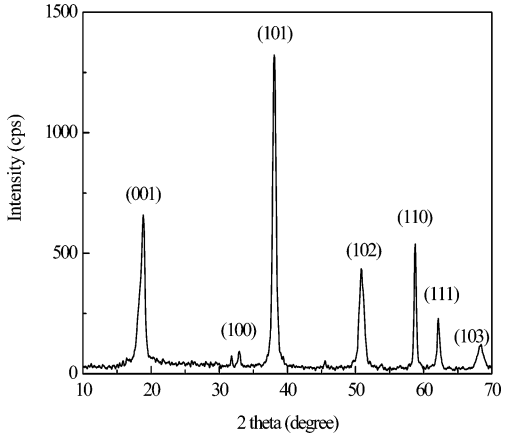


**Figure 6.** XRD analysis of produced $Mg(OH)_2$ particles. Operating conditions: $[MgCl_2] = 0.83$ M, $[NaOH] = 1.66$ M, $L_1 = L_2 = 0.28$ L/min, and $N = 2000$ rpm.

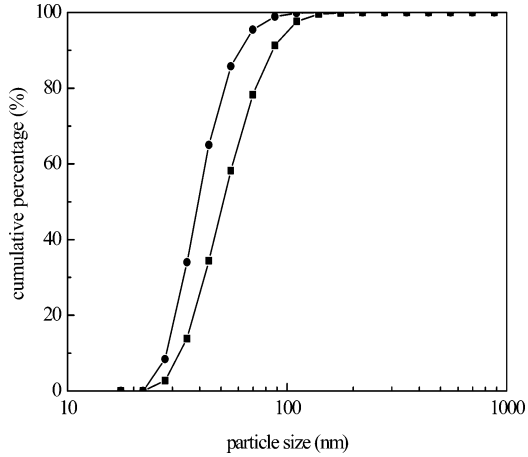


**Figure 7.** Cumulative particle size distribution of $Mg(OH)_2$ on a number basis (●) and volume basis (■). Specific conditions: $[MgCl_2] = 0.83$ M, $[NaOH] = 1.66$ M, $L_1/L_2 = 1/1$, and $N = 2000$ rpm.

very far from 10.0, was caused by the excess NaOH. Figure 2 shows SEM micrographs of $Mg(OH)_2$ particles produced at different $[MgCl_2]/[NaOH]$ ratios. In Figure 2a,c, the $Mg(OH)_2$ particles are very small, and few aggregates are observed. On the other hand, when the ratio was 1/4, excess NaOH caused some aggregation. Some large aggregates with sizes between 1 and 10 $\mu$m can be seen in Figure 2b. They could not be dispersed, even by using a sonicator. The reason for this result might be as follows. The solubility of $Mg(OH)_2$ under the very high pH value was lower than that at pH 10, and this caused a larger driving force for nucleation. After the extremely fast nucleation, the small nuclei were immediately negatively charged by adsorption of $OH^-$ ions under the strong basic conditions, and they interconnected with each other through hydrogen bonds, resulting in agglomerations.[24]

**3.4. Effects of Magnesium Source on $Mg(OH)_2$ Morphology.** Many magnesium compounds have been used as magnesium sources for producing magnesium hydroxide, such as a salt consisting of magnesium chloride, nitrate, and sulfate, and different morphologies resulting from different sources have been reported.[1] In this experiment, two magnesium salts, $MgCl_2 \cdot 6H_2O$ and $MgSO_4 \cdot 7H_2O$, were used to study their effects on the $Mg(OH)_2$ morphology. The concentrations used for $MgCl_2 \cdot 6H_2O$ and $MgSO_4 \cdot 7H_2O$ were 0.83 and 0.80 M, respectively. The other operating conditions were the same in Figure 2a. The pH value of the exit stream from the reactor for $MgSO_4 \cdot 7H_2O$ was 9.7, which was somewhat lower than that for $MgCl_2 \cdot 6H_2O$, which was 10.0. The FEG-SEM micrographs from this experiment are shown in Figure 3. As shown in Figure 3a, lamellar-like $Mg(OH)_2$ particles randomly piled up when $MgCl_2 \cdot 6H_2O$ was used as the magnesium source. This result was very different from that obtained using $MgSO_4 \cdot 7H_2O$ as the magnesium source, as seen in Figure 3b, which shows an intergrowth structure like a "sand rose." This result is similar to that reported by Henrist et al.,[1] who reacted $MgSO_4$ with $NH_4OH$. It is conjectured that the $SO_4^{2-}$ ion might be responsible for this peculiar structure. These small platelets, connected to each other, did not pile up in parallel, but at peculiar angles and looked like they grew simultaneously from preagglomerated nuclei.

**3.5. Effects of Reactant Flow Rate on $Mg(OH)_2$ Particle Size.** The mass-transfer rate and micromixing in the high-gravity equipment depend heavily on the liquid flow rate.[16−18,25] In this experiment with the concentration of $MgCl_2$ fixed at 0.83 M, the concentration of NaOH at 1.66 M, and the rotation speed at 2000 rpm, the liquid flow rates of both reactant solutions were changed simultaneously from 0.28 to 0.75 L/min to see how they would affect the $Mg(OH)_2$ particle size. The results are shown in Figure 4, which shows that when the liquid flow rate was increased from 0.28 to 0.75 L/min, the volume mean size of the magnesium hydroxide increased substantially from 62.7 to 195.5 nm, and the number mean size increased from 47.5 to 143.6 nm. It was understood that the increase in the liquid flow rate resulted in a thicker liquid film on the spinning disk. Thus, the mixing between the two reactant solutions was poor and

**Table 1. Calcination Temperature Programs for Producing MgO from $Mg(OH)_2$[a]**

| program no. | calcination temperature program | final calcination temp (°C) |
|---|---|---|
| 1 | constant temperature at 25 °C | 25 |
| 2 | 25 °C → 100 °C (0.5 h) → 280 °C (1 h) | 280 |
| 3 | 25 °C → 100 °C (0.5 h) → 450 °C (2 h) | 450 |
| 4 | 25 °C → 100 °C (0.5 h) → 280 °C (1 h) → 450 °C (2 h) | 450 |
| 5 | 25 °C → 100 °C (0.5 h) → 280 °C (1 h) → 450 °C (2 h) → 600 °C (2 h) | 600 |
| 6 | 25 °C → 100 °C (0.5 h) → 350 °C (1 h) → 450 °C (2 h) → 800 °C (2 h) | 800 |

[a] The rate of temperature increase was 10 °C/min, and the holding times are shown in parentheses following the temperatures.

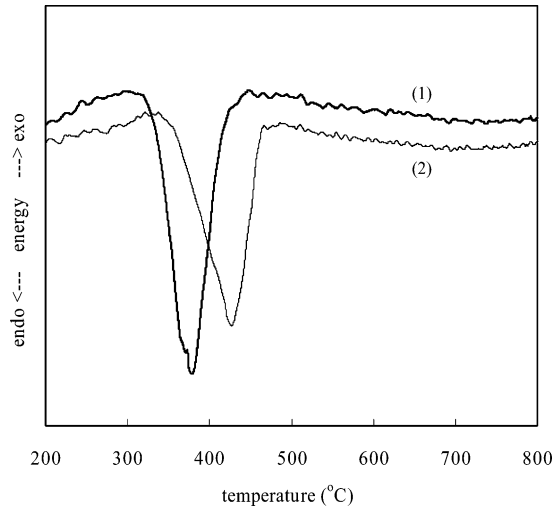


**Figure 8.** DTA analysis of $Mg(OH)_2$: curve 1, produced nanoparticles shown in Figure 6; curve 2, submicron particles from Nacalai Tesque.

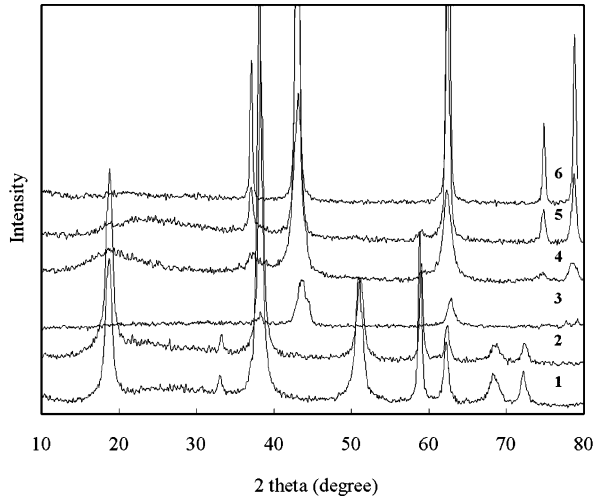


**Figure 9.** XRD analysis of $Mg(OH)_2$ calcined under various temperature programs shown in Table 1.

the reaction might not be completed on the disk. The residual reactants finally reacted in the collection vessel, where the crystals grew to form larger particles with a wider distribution.[26] Figure 5 clearly shows the results for the cumulative particle size distributions under the two reactant flow rates, i.e., 0.28 and 0.75 L/min. The particle size was larger, and the size distribution was wider, for the sample obtained at the higher flow rate.

**3.6. Analysis of the Produced $Mg(OH)_2$ Powder.** The produced $Mg(OH)_2$ with the smallest size was subjected to the following analyses: XRD, FEG-SEM, DTA, and BET surface area. Figure 6 shows the results of XRD analysis of the sample, which indicates a hexagonal structure. The crystallite size estimated using the Debye−Scherrer formula based on the full width at half-maximum of the diffraction peak was 14.5 nm. The FEG-SEM micrograph shown in Figure 3a reveals that the

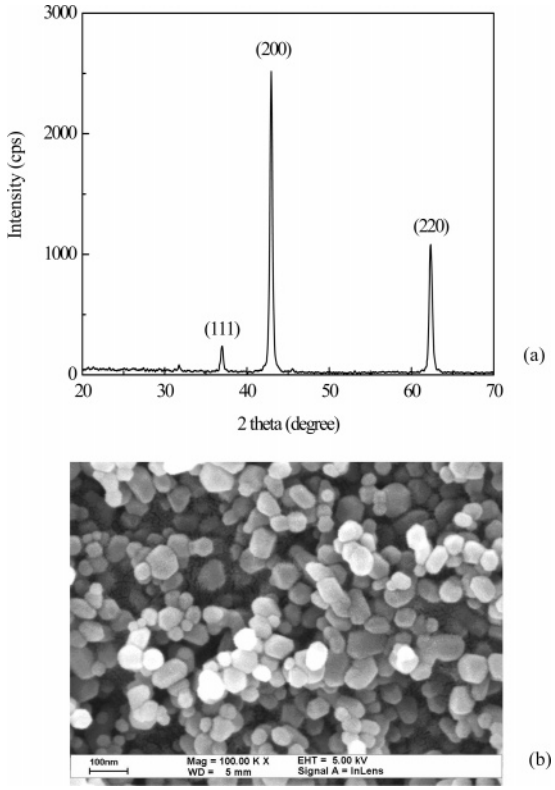


**Figure 10.** (a) XRD analysis and (b) FEG-SEM micrograph of MgO calcined from $Mg(OH)_2$ produced by a spinning disk reactor.

morphology of $Mg(OH)_2$ was lamellar-like, 50−80 nm in width and about 10 nm thick. The BET specific surface area was 77 $m^2/g$, equivalent to a sphere of 32.8 nm in diameter. The mean particle size based on number measured with a dynamic light scattering analyzer was 47.5 nm. The cumulative size distribution is shown in Figure 7. It can be seen in Figure 7 that the particle size of the $Mg(OH)_2$ produced with the SDR was between 20 and 200 nm, and the percentage of $Mg(OH)_2$ particles smaller than 100 nm was greater than 98%, which meets the requirement of a nanoscale powder.

**3.7. Calcination of $Mg(OH)_2$ To Prepare MgO.** In order to find a suitable calcination temperature for producing MgO powder, the produced $Mg(OH)_2$ sample was analyzed with DTA to find the dehydration temperature of $Mg(OH)_2$. The results of DTA are shown in Figure 8 (curve 1). The dehydration temperature was found to be 379 °C. A similar curve of $Mg(OH)_2$ powder purchased from Nacalai Tesque is also presented in Figure 8 (curve 2). The dehydration temperature of this powder sample with a size range between 200 and 500 nm was about 45 °C higher than that of the produced powder, which was about 1/10 in size. In addition, the endothermic peak of the sample produced at the dehydration temperature was higher. This meant that nanosized $Mg(OH)_2$ could dehydrate at a lower temperature and absorb more heat energy than submicron particles of the same weight, showing its potential as a superior flame retardant material.[27]

Since the dehydration temperature of $Mg(OH)_2$ produced in this experiment was about 379 °C, a calcination temperature higher than that would give MgO. Several calcination temperature programs for producing MgO, shown in Table 1, were designed to find the most appropriate one, and these programs were similar to that presented by Ding et al.,[7] in which the rate of temperature increase was 10 °C/min and the temperature was held at 100 °C for 0.5 h to remove moisture, at 280 °C for 1 h to remove impurities, at 450 °C for 2 h to completely dehydrate the $Mg(OH)_2$, and at 600 °C for 2 h to enhance the crystal structure of the MgO. The XRD results for the calcinated samples are shown in Figure 9. It can be seen that MgO appeared at 450 °C but its crystal structure was not well-developed. When the final calcination temperature was higher than 600 °C, the XRD patterns showed strong diffraction peaks of MgO, which enabled us to calculate the crystallite sizes, i.e., 16.0 and 29.2 nm for 600 °C (program 5) and 800 °C (program 6), respectively. The size data revealed that the crystallite size increased with the increase in the final calcination temperature. In order to obtain smaller MgO particles with well-developed crystal structures, program 5 was chosen for the study of MgO characterization.

The calcined powder had a standard cubic crystal structure as determined through XRD, and the results are shown in Figure 10a, from which the crystallite size was calculated as 26.7 nm. The FEG-SEM micrograph shown in Figure 10b reveals that polyhedral MgO particles, 30−70 nm in diameter with some degree of aggregation, were obtained. The aggregation of particles caused the volume mean size to be 150 nm as measured with a dynamic light scattering analyzer.

## 4. Conclusions

In this study, magnesium hydroxide nanoparticles were successfully synthesized using a spinning disk reactor. The produced magnesium hydroxide particles were round and disk-shaped, 50−80 nm in diameter and 10 nm thick, and the BET surface area was 77 $m^2/g$. Several operating variables that affected the particle size were investigated, including the reactant concentration, the rotation speed of the spinning disk, the concentration ratio of magnesium salt to sodium hydroxide, and the flow rates of the reactant solutions, among which the last two variables were the most significant factors. For example, the number mean size of $Mg(OH)_2$ particles increased from 47.5 to 143.6 nm when the flow rate of the reactant solution increased from 0.28 to 0.75 L/min. Polyhedral nanoparticles of 30−70 nm magnesium oxide, examined under a scanning electron microscope, were obtained by calcining the 47.5 nm $Mg(OH)_2$ powder of lamellar shape, using a heating program with temperatures up to 600 °C. DTA of the produced $Mg(OH)_2$ sample showed that this material has great advantages when applied as a flame retardant. This research shows that the spinning disk reactor is a powerful tool for producing nanoparticles and has great potential in commercialization.

## Acknowledgment

The authors wish to thank the National Science Council of Taiwan for financial support of this work.

## Literature Cited

(1) Henrist, C.; Mathieu, J. P.; Vogels, C.; Rulmont, A.; Cloots, R. Morphological study of magnesium hydroxide nanoparticles precipitated in dilute aqueous solution. *J. Cryst. Growth* **2003**, *249*, 321.

(2) Booster, J. L.; Van Sandwijk, A.; Reuter, M. A. Conversion of magnesium fluoride to magnesium hydroxide. *Miner. Eng.* **2003**, *16*, 273.

(3) Phillips, V. A.; Kolbe, J. L.; Opperhauser, H. Effect of pH on the growth of $Mg(OH)_2$ crystals in an aqueous environment at 60 °C. *J. Cryst. Growth* **1977**, *41*, 228.

(4) Donnary, J. D. H. *Crystal data: determinative tables*, 3rd ed; National Bureau of Standards: Washington, DC, 1972.

(5) Lv, J.; Qiu, L.; Qu, B. Controlled growth of three morphological structures of magnesium hydroxide nanoparticles by wet precipitation method. *J. Cryst. Growth* **2004**, *267*, 676.

(6) Yu, J. C.; Xu, A.; Zhang, L.; Song, R.; Wu, L. Synthesis and characterization of porous magnesium hydroxide and oxide nanoplates. *J. Phys. Chem. B* **2004**, *108*, 64.

(7) Ding, Y.; Zhang, G.; Wu, H.; Hai, B.; Wang, L.; Qian, Y. Nanoscale magnesium hydroxide and magnesium oxide powders: control over size, shape, and structure via hydrothermal synthesis. *Chem. Mater.* **2001**, *13*, 435.

(8) Wang, J. A.; Novaro, O.; Bokhimi, X.; López, T.; Gómez, R.; Navarrete, J.; Llanos, M. E.; López-Salinas, E. Characterizations of the thermal decomposition of brucite prepared by sol-gel technique for synthesis of nanocrystalline MgO. *Mater. Lett.* **1998**, *35*, 317.

(9) Utamapanya, S.; Klabunde, K. J.; Schlup, J. R. Nanoscale metal oxide particles/clusters as chemical reagents. Synthesis and properties of ultrahigh surface area magnesium hydroxide and magnesium oxide. *Chem. Mater.* **1991**, *3*, 175.

(10) Sorrell, C. A. *A guide to field identification: Rocks and Minerals*; Golden Press: New York, 1973.

(11) Ardizzone, S.; Bianchi, C. L.; Vercelli, B. Structural and morphological features of MgO powders. The key role of the preparative starting compound. *J. Mater. Res.* **1998**, *13* (8), 2218.

(12) Choudhary, V. R.; Rane, V. H.; Gadre, R. V. Influence of precursors used in preparation of MgO on its surface properties and catalytic activity in oxidative coupling of methane. *J. Catal.* **1994**, *145*, 300.

(13) Jost, H.; Braun, M.; Carius, Ch. The role of reactivity in syntheses and the properties of magnesium oxide. *Solid State Ionics* **1997**, *101−103*, 221.

(14) Ramshaw, C.; Mallinson, R. H. Mass Transfer Process. U.S. Patent 4,383,255, 1981.

(15) Kelleher, T.; Fair, J. R. Distillation studies in a high-gravity contactor. *Ind. Eng. Chem. Res.* **1996**, *35*, 4646.

(16) Lin, C. C.; Liu, H. S. Adsorption in a centrifugal field: basic dye adsorption by activated carbon. *Ind. Eng. Chem. Res.* **2000**, *39*, 161.

(17) Chen, Y. S.; Liu, H. S. Absorption of VOCs in a rotating packed bed. *Ind. Eng. Chem. Res.* **2002**, *41*, 1583.

(18) Lin, C. C.; Liu, W. T.; Tan, C. S. Removal of carbon dioxide by absorption in a rotating packed bed. *Ind. Eng. Chem. Res.* **2003**, *42*, 2381.

(19) Chen, J. F.; Wang, Y. H.; Guo, F.; Wang, X. M.; Zheng, C. Synthesis of nanoparticles with novel technology: high-gravity reactive precipitation. *Ind. Eng. Chem. Res.* **2000**, *39*, 948.

(20) Song, Y. H.; Chen, C. M.; Chen, C. F. China Patent 01141787.0, CN 1341694A, 2002.

(21) Cafiero, L. M.; Baffi, G.; Chianese, A.; Jachuck, R. J. J. Process intensification: precipitation of barium sulfate using a spinning disk reactor. *Ind. Eng. Chem. Res.* **2002**, *41*, 5240.

(22) Mohanty, R.; Bhandarkar, S.; Zuromski, B.; Brown, R.; Estrin, J. Characterizing the product crystals from a mixing Tee process. *AIChE J.* **1988**, *34* (12), 2063.

(23) Chen, C. K. Crystal morphology control of nano-/micro-sized calcium carbonate using reverse microemulsion technique. Master's Thesis, Department of Chemical Engineering, National Taiwan University, Taiwan, 2004.

(24) Tang, F. Q.; Huang, X. X.; Zhang, Y. F.; Guo, J. K. Effect of dispersants on surface chemical properties of nano-zirconia suspensions. *Ceram. Int.* **2000**, *26*, 93.

(25) Liu, H. S.; Lin, C. C.; Wu, S. C.; Hsu, H. W. Characteristics of a rotating packed bed. *Ind. Eng. Chem. Res.* **1996**, *35*, 3590.

(26) Tai, C. Y.; Chien, W. C.; Chen, P. C. Particle nucleation and growth. *Encyclopedia of Surface and Colloid Science*; Marcel Dekker, Inc.: New York, 2002; p 3903.

(27) Zhang, Q.; Tian, M.; Wu, Y.; Lin, G.; Zhang, L. Effect of particle size on the properties of $Mg(OH)_2$-filled rubber composites. *J. Appl. Polym. Sci.* **2004**, *94*, 2341.

*Received for review* July 6, 2006
*Revised manuscript received* May 28, 2007
*Accepted* June 13, 2007

IE060869B